

A Mössbauer investigation of nano-NiFe alloy/expanded graphite for electromagnetic shielding

Wei Liu¹ · Yu-An Huang² · Lai Wei¹ · Ya Zhai³ · Rui-Li Zhang¹ ·
Tao Tang¹ · Run-Sheng Huang¹

Received: 29 April 2015/Revised: 27 October 2015/Accepted: 9 November 2015/Published online: 17 September 2016
© Shanghai Institute of Applied Physics, Chinese Academy of Sciences, Chinese Nuclear Society, Science Press China and Springer Science+Business Media Singapore 2016

Abstract A new material is prepared by impregnating the expanded graphite (EG) into ethanol solutions of metal acetate and then drying and reducing it in H₂. It contains the EG and the nanoparticles of the magnetic Ni–Fe alloy for the electromagnetic shielding. Its morphology, phase structure, magnetic properties, and electromagnetic shielding effectiveness (SE) are investigated in our experiment. It shows that the morphology, the phase structure, and the magnetic property of the composite can be modified by altering the Ni content in the alloy nanoparticles. Interestingly, the SE can be enhanced to 54–70 dB at low frequencies (300 kHz–10 MHz) by dispersing the magnetic nanoparticles onto EG.

Keywords Expanded graphite · Nano-NiFe alloy · Electromagnetic shielding · Mössbauer spectra

This work was supported by the National Natural Science Foundation of China (Nos. 50977042 and 10904061), the “863” program of MSTC (No. 2006AA03Z458) and the research funds for Nanjing Institute of Technology (No. YKJ201002).

✉ Run-Sheng Huang
rhuang@nju.edu.cn

- ¹ School of Physics, Nanjing University, Nanjing 210093, China
- ² Department of Material Engineering, Nanjing Institute of Technology, Nanjing 211167, China
- ³ Department of Physics, Southeast University, Nanjing 211102, China

1 Introduction

Ferromagnetic nanoparticles have potential applications in magnetic fluids [1, 2], catalysts [3], and biomaterials [4]. It can also be used as the electromagnetic radiation shielding material [5]. These kind of metal nanoparticles can also be deposited on some carriers with a large surface area for special applications. The expanded graphite (EG), one of the high applicable carriers, has abundant pores and gaps to embed nanoparticles [6]. Due to its excellent electrical conductivity, EG possesses high electromagnetic shielding effectiveness (SE) in the range of 1–2 GHz. But its SE is not satisfactory at lower frequencies [7–10] at this moment. Alternatively, the SE of materials can be improved by loading magnetic metal nanoparticles onto EG since their magnetic particles exhibit the better conductivity and a magnetic property as well.

The previous works have provided a method by evaporating and depositing the Ni_x–Fe_{1–x} alloy nanoparticles in the atmosphere of nitrogen. Meanwhile, a chemical method [8–12] has been used to prepare the composites with nanosized Co or Ni particles evenly dispersed on the surface of EG. In this paper, a method to disperse Ni and Fe nanoparticles on EG by using chemical methods is introduced, and the SE of the composites is measured. At the same time, the morphology, phase structure, and magnetic property of the composites are studied.

2 Experimental details

EG was prepared by heating about 3 g commercial expandable graphite intercalated by H₂SO₄ in a microwave oven at 900 W for 3 min. It was then added into an ethanol

Fig. 1 Typical SEM images of
a Ni_{1.00}-Fe_{0.00}-70 %EG,
b Ni_{0.00}-Fe_{1.00}-70 %EG,
c Ni_{0.35}-Fe_{0.65}-70 %EG,
d Ni_{0.60}-Fe_{0.40}-70 %EG

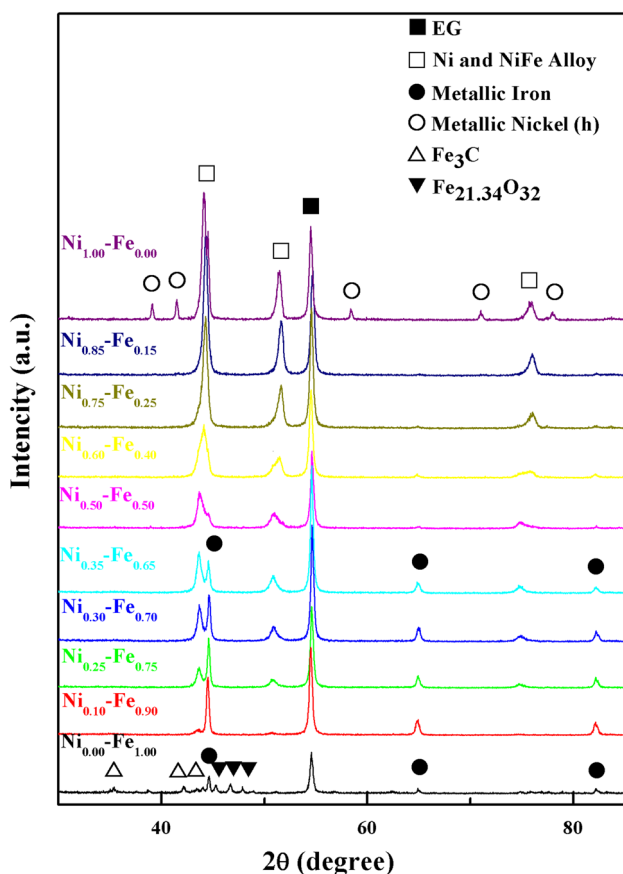
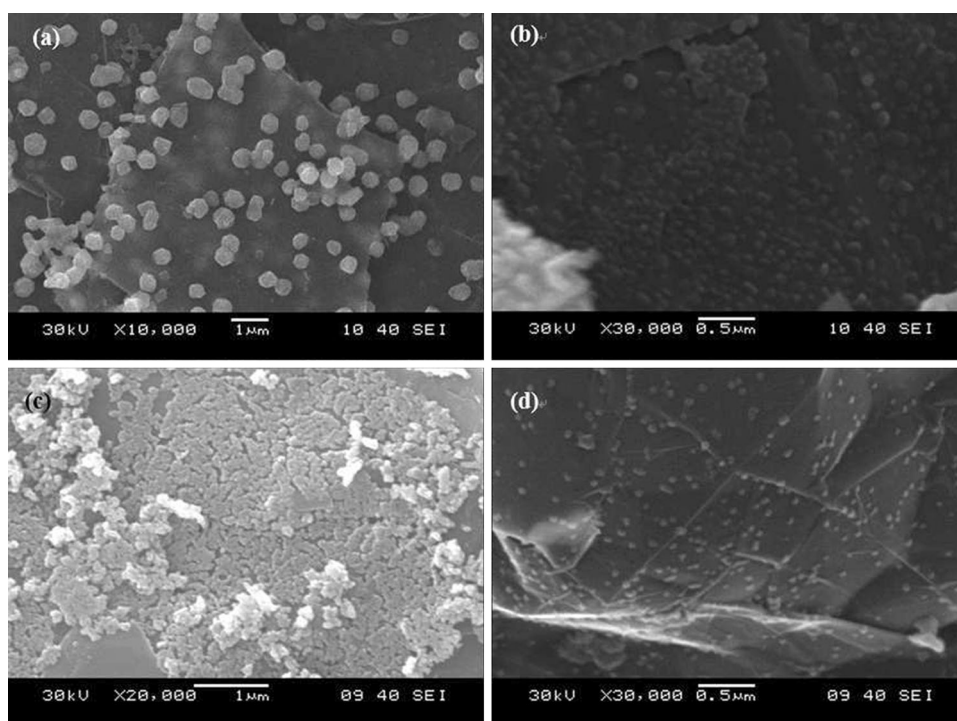


Fig. 2 XRD patterns of the samples of nano-NiFe alloy/EG at different x values

solution containing a certain amount of iron nitrate, nickel acetate, and acetic acid as well. After heating the mixture in a water bath at 353 K to evaporate the solvent, the composite was then reduced in a H₂ flow at 723 K for 600 min. Finally, the composite was obtained by cooling it in N₂. Some earlier works pointed out that the composite material has better SE while the weighted content of the metal nanoparticles is about 30 %. So we set the mass fraction of Ni-Fe at 30 % and merely changed the Ni mole content x in the Ni _{x} -Fe_{1- x} nanoparticles ($x = 0.00, 0.10, 0.25, 0.30, 0.35, 0.50, 0.60, 0.75, 0.85, 1.00$) to study the effect of the mole content of Ni in the mixed metals.

Scanning electron microscopy (SEM) micrographs were obtained by using a JEOL JSM-6380LV microscope. X-ray powder diffraction (XRD) patterns were recorded in the range of 2θ from 30° to 85° on a D8 ADVANCE (Bruker, Germany) diffractometer operating at 40 kV with Cu K _{α} radiation ($\lambda = 1.5418\text{\AA}$). The Mössbauer spectra were recorded on a Wissel Mössbauer spectrometer (radioactive source: ⁵⁷Co/Rh). The static magnetic properties were characterized by a vibrating sample magnetometer (VSM) operating at the room temperature. All the samples were, respectively, pressed under 10 MPa to form the annular rings with the inner and outer diameters of 12 and 115 mm. Then, the electromagnetic SE was measured by a network analyzer (Agilent E5062A) in the frequency ranged from 300 kHz to 1.5 GHz [13] by the standard ASTM D4935 [14].

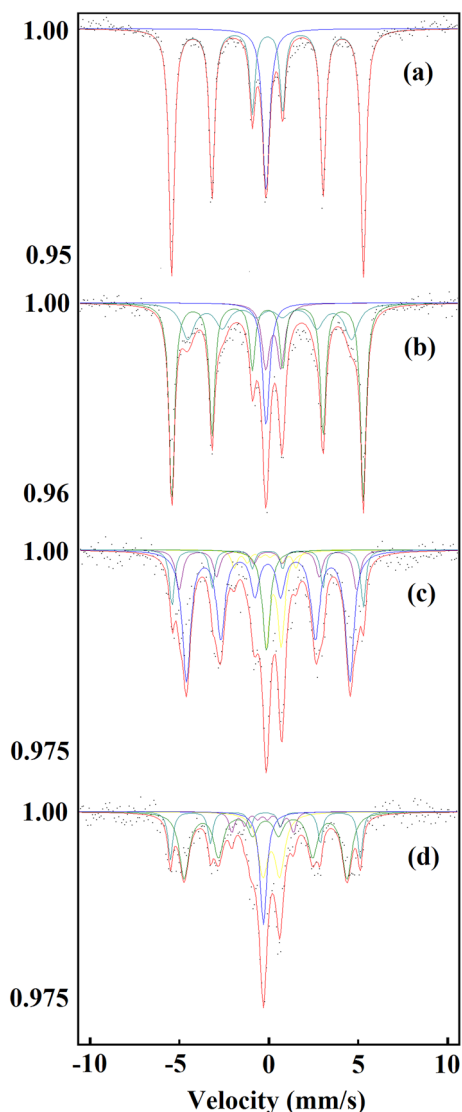


Fig. 3 Mössbauer spectrum of nano-NiFe alloy/EG at different Ni contents. *a* Ni_{0.10}-Fe_{0.90}-EG, *b* Ni_{0.30}-Fe_{0.70}-EG, *c* Ni_{0.50}-Fe_{0.50}-EG, *d* Ni_{0.60}-Fe_{0.40}-EG

3 Results and discussion

SEM was used to observe the morphologies of the composites prepared in our work. Figure 1a, b shows that the metallic Ni or Fe particles are formed and spread separately on the surfaces of the EG layers in the composites of Ni_{1.00}-Fe_{0.00}-EG and Ni_{0.00}-Fe_{1.00}-EG, respectively. The Ni particles (Fig. 1a) are generally spherical in shape but with tiny edges and corners, while Fe particles (Fig. 1b) are rounder. The sphere structure has sizes around 100–500 nm. According to the SEM images of the samples with other Ni contents, when the amount of Ni is less than that of Fe, the agglomerative distributions are like fish scales. Otherwise, the distributions are separate and homogeneous, as shown in Fig. 1c, d.

The phase of the products was investigated by XRD and Mossbauer spectrometer. In Fig. 2, the XRD results show clearly the strong diffraction peaks in EG and the metals. According to the XRD database, the 2θ of XRD peaks for Ni, Fe, and Ni-Fe alloy are all close to 44.5° , 51.8° , and 76.4° . So the formation of Ni_{*x*}-Fe_{1-*x*} alloy cannot be confirmed definitely here. However, we can find other weak peaks corresponding to the hexagonal structure of metallic Ni in Ni_{1.00}-Fe_{0.00}-EG. In addition, the weak diffraction peaks for Fe₃C and ferric oxide are observed in the composite Ni_{0.00}-Fe_{1.00}-EG. We believe that C and Fe could easily form a solid solution under a high temperature, and the ferric oxide is formed by the passivation in a cooling process.

Mössbauer spectra have been used to further analyze the formation of numerous iron-containing compounds [15, 16]. Considering the minimum atomic concentration value of Fe in Mössbauer measurement condition, Ni_{*x*}-Fe_{1-*x*}-EG ($x = 0.10, 0.30, 0.50, 0.60$) were chosen as the experimental samples. The spectra are shown in Fig. 3. All these spectra can be separated into the several magnetic, paramagnetic, or nonmagnetic phases. With decrease in the Fe content, the percentage of α -Fe phase descends quickly, and several other phases of the alloy increase. Although the exact composition remains uncertain, the singlets in the middle, which corresponds to the paramagnetic phase, appear in all spectra. Nowadays, there exist two main views about the paramagnetic phases in Fe-Ni alloys: One is the small quantity of *fcc* structure [17, 18], and another is the low-spin γ_{LS} -Ni-Fe by the meteoritic study [19, 20]. Three kinds of sextets show the different components of Fe in Fe-Ni alloy. They are $\gamma(\text{Fe, Ni})$ with the hyperfine field of 28.65 or 31.14 T and FeNi₃, in which the $\gamma(\text{Fe, Ni})$ phase with 28.65 T dominates. The total area of $\gamma(\text{Fe, Ni})$ phase displays a tendency of an increase and then decreases with the decrease in Fe content. All these sextets possess a higher line width, which is due to the character of a distribution of hyperfine fields. This fact also hints at the existence of the different type of Ni-Fe coordination and thus the magnetic ordering. When the ferric content is <70 % of the metal, the sub-spectrum of the ferric oxide indicates the passivation to cause Fe coated by the metal oxide film. The complete parameters of sub-spectra of Mössbauer are given in Table 1.

The magnetic hysteresis loops of the composites were measured at room temperature. The specific saturation and remnant magnetization, the coercivity, and the ratios of remnant to saturation magnetization (σ_r/σ_s) of composites are all displayed in Table 2. Due to the nanometer sizes, the specific saturation magnetic moments of the metallic Ni and Fe nanoparticles in the composites Ni_{1.00}-Fe_{0.00}-EG and Ni_{0.00}-Fe_{1.00}-EG are obviously smaller than that of the

Table 1 Sub-spectrum parameters of Mössbauer spectrum of nano-NiFe alloy/EG at different Ni contents

Samples	Fe site	Area (%)	W (mm/s)	IS (mm/s) ^a	QS (mm/s)	H (T)
Ni _{0.10} -Fe _{0.90}	Sextet	81.97 ^b	0.35	0		33.11
Ni _{0.10} -Fe _{0.90}	Singlet	18.03 ^c	0.47	-0.233		
Ni _{0.30} -Fe _{0.70}	Sextet	54.30 ^b	0.38	0		33.12
Ni _{0.30} -Fe _{0.70}	Sextet	23.60 ^d	0.50	-0.135		28.65
Ni _{0.30} -Fe _{0.70}	Doublet	11.50 ^e	0.41	0.185	0.867	
Ni _{0.30} -Fe _{0.70}	Singlet	10.60 ^c	0.47	-0.233		
Ni _{0.50} -Fe _{0.50}	Sextet	12.07 ^b	0.32	0		33.16
Ni _{0.50} -Fe _{0.50}	Sextet	48.72 ^d	0.47	-0.145		28.65
Ni _{0.50} -Fe _{0.50}	Sextet	11.69 ^e	0.44	-0.136		31.14
Ni _{0.50} -Fe _{0.50}	Sextet	4.47 ^f	0.38	-0.293		10.83
Ni _{0.50} -Fe _{0.50}	Doublet	14.47 ^g	0.48	0.186	0.856	
Ni _{0.50} -Fe _{0.50}	Singlet	8.55 ^c	0.52	-0.233		
Ni _{0.30} -Fe _{0.70}	Sextet	15.75 ^b	0.33	0		33.09
Ni _{0.30} -Fe _{0.70}	Sextet	43.71 ^d	0.55	-0.141		28.65
Ni _{0.30} -Fe _{0.70}	Sextet	7.24 ^f	0.35	-0.309		10.84
Ni _{0.30} -Fe _{0.70}	Doublet	20.24 ^g	0.47	0.176	0.947	
Ni _{0.30} -Fe _{0.70}	Singlet	12.81 ^c	0.46	-0.261		

^a Isomer shift value is relative to α -Fe

^b Corresponding to α -Fe

^c Corresponding to the paramagnetic phase of Ni-Fe

^d Corresponding to one of the γ (Fe, Ni) phases

^e Corresponding to another γ (Fe, Ni) phase

^f Corresponding to FeNi₃

^g Corresponding to ferric oxide

Table 2 Static magnetic parameter of nano-NiFe alloy/EG at different Ni contents

Ni content	σ_s (emu/g)	σ_r (emu/g)	H_c (Oe)	σ_r/σ_s
0	134.3	30.5	442	0.227
0.10	141.5	16.6	204	0.117
0.25	149.6	33.4	296	0.223
0.30	133.5	40.6	345	0.304
0.35	123.2	41.4	331	0.336
0.50	139.8	70.6	468	0.505
0.60	116.1	38.5	283	0.332
0.75	82.6	32.5	296	0.393
0.85	52.1	18.2	233	0.349
1.00	30.1	3.5	93	0.116

corresponding bulk metals. For Ni_{0.00}-Fe_{1.00}-EG, the diamagnetic nature of the coexisted metal carbides also decreases the values. When the Ni content is less than Fe, the saturation moments of mixed metals are generally even larger than that of pure Fe in nanoscale, which might be due to the formation of Fe-Ni alloy. In addition, σ_r/σ_s for the nanoparticles in EG are found to be from 0.12 to 0.50, indicating their soft magnetic nature.

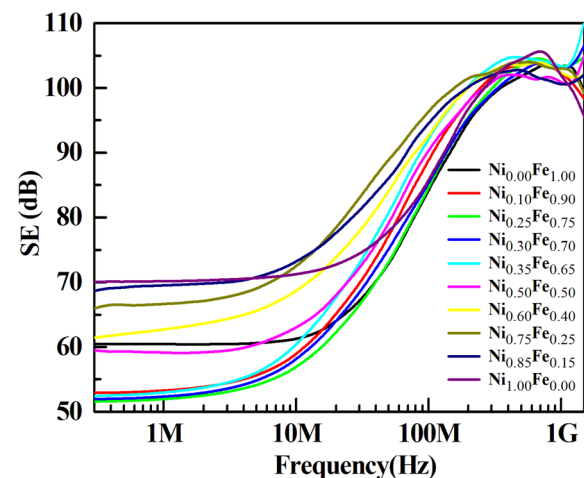
**Fig. 4** SE of the composites Ni_x-Fe_{1-x}-EG for electromagnetic shielding at the frequencies from 300 kHz to 1.5 GHz

Figure 4 presents the SE of the composite Ni_x-Fe_{1-x}-EG. It is demonstrated that the SE of EG at lower frequencies is clearly improved based on the fact that Ni and Fe magnetic nanoparticles are loaded on it. Consequently, the SE values of the composites are prompted to 54–70 dB at the frequency of 300 kHz. However, it contributes very

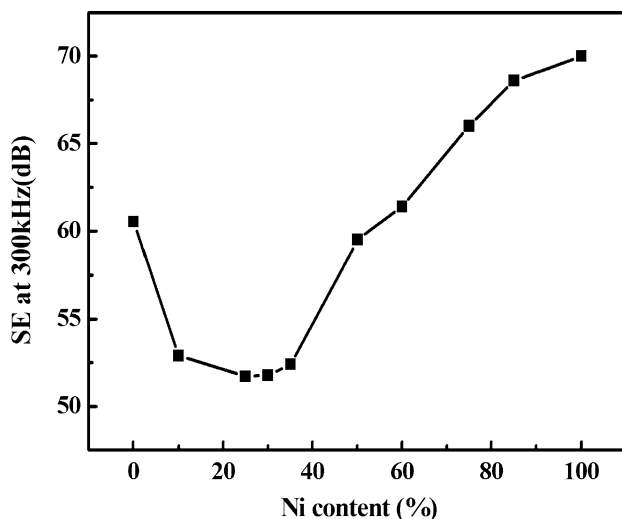


Fig. 5 Effect of Ni content on the SE of the composites Ni_x-Fe_{1-x} -EG at 300 kHz

little at higher frequencies to load magnetic particles on EG. Specifically, it remains about 105 dB in the range of 1–1.5 GHz. The reason might be that the presence of metal particles and the solution harm the surface of EG, causing the reflection loss to decrease at higher frequencies. Furthermore, the content of Ni has a significant effect on the SE of the composite at 300 kHz, which is depicted in Fig. 5. When the amount of Ni is less than that of Fe, the SE values at 300 kHz are not as good as expected; the minimum is occurred at $x = 0.25-0.30$. Possibly, the behavior of a super-paramagnetic state happens when x is near by 0.30 [21]. Another possible reason is that the agglomerations of the metal particles turn out to harm the original layer structure of EG and reduce its electric conductivity. While $x > 0.50$, the SE increases with the Ni content and finally reaches to the maximum value 70 dB when the Ni content is 1.00.

4 Conclusion

In this work, the magnetic Fe and Ni nanoparticles are dispersed on EG by impregnating EG into the ethanol solution of metal acetates, followed by drying and reducing in H_2 . When the Ni content is less than Fe (except $x = 0$), the metal particles distribute agglomeratively. Otherwise, they distribute separately. The Mössbauer spectra are clearly showing the change of Ni–Fe phases with the content of Ni. At the frequency of 300 kHz, the SE values are prompted to 54–70 dB. In particular, the minimum SE value 54 dB occurs at $x = 0.25-0.30$, and the SE at 300 kHz increases with Ni content when $x > 0.50$. At the end, the composite only with Ni in EG ($x = 1.00$) reaches

the SE of 70–105 dB in the frequency range from 300 kHz to 1.5 GHz.

References

1. M. Xiong, Y. Gao, J. Liu, Fabrication of magnetic nano liquid metal fluid through loading of Ni nanoparticles into gallium or its alloy. *J. Magn. Magn. Mater.* **354**, 279–283 (2014). doi:10.1016/j.jmmm.2013.11.028
2. S. Panday, B.S.S. Daniel, P. Jeevanandam, Synthesis of nanocrystalline CoNi alloys by precursor approach and studies on their magnetic properties. *J. Magn. Magn. Mater.* **323**, 2271–2280 (2011). doi:10.1016/j.jmmm.2011.04.006
3. S. de Llobet, J.L. Pinilla, R. Moliner et al., Effect of the synthesis conditions of Ni/Al_2O_3 catalysts on the biogas decomposition to produce H_2 -rich gas and carbon nanofibers. *Appl. Catal. B Environ.* **165**, 457–465 (2015). doi:10.1016/j.apcatb.2014.10.014
4. S.H. Chang, B.Y. Chen, Y.C. Lin, Toxicity assessment of three-component Fe–Cr–Ni biomedical materials using an augmented simplex design. *Mater. Sci. Eng. C* **32**, 1893–1896 (2012). doi:10.1016/j.msec.2012.05.008
5. X. Yu, Z. Shen, The electromagnetic shielding of Ni films deposited on cenosphere particles by magnetron sputtering method. *J. Magn. Magn. Mater.* **321**, 2890–2895 (2009). doi:10.1016/j.jmmm.2009.04.040
6. G. Shi, W. Li, Y. Lu, Fe-based surface activator for electroless nickel deposition on polyester: application to electromagnetic shielding. *Surf. Coat. Technol.* **253**, 221–226 (2014). doi:10.1016/j.surfcoat.2014.05.040
7. S.R. Dhakate, S. Sharma, M. Borah et al., Expanded graphite-based electrically conductive composites as bipolar plate for PEM fuel cell. *Int. J. Hydrogen Energy* **33**, 7146–7152 (2008). doi:10.1016/j.ijhydene.2008.09.004
8. X. Luo, D.D.L. Chung, Electromagnetic interference shielding reaching 130 dB using flexible graphite. *Carbon* **34**, 1293–1294 (1996). doi:10.1016/0008-6223(96)82798-9
9. Y. Huang, Z. Xu, J. Shen et al., Dispersion of magnetic metals on expanded graphite for the shielding of electromagnetic radiations. *Appl. Phys. Lett.* **90**, 133117 (2007). doi:10.1063/1.2718269
10. Z. Xu, Y. Huang, Y. Yang et al., Dispersion of iron nano-particles on expanded graphite for the shielding of electromagnetic radiation. *J. Magn. Magn. Mater.* **322**, 3084–3087 (2010). doi:10.1016/j.jmmm.2010.05.034
11. X. Yu, Z. Shen, C. Cai, Millimeter wave electromagnetic interference shielding by coating expanded polystyrene particles with a copper film using magnetron sputtering. *Vacuum* **83**, 1438–1441 (2009). doi:10.1016/j.vacuum.2009.05.021
12. M. Mishra, A.P. Singh, S.K. Dhawan, Expanded graphite–nanoferrite–fly ash composites for shielding of electromagnetic pollution. *J. Alloy. Compd.* **557**, 244–251 (2013). doi:10.1016/j.jallcom.2013.01.004
13. X. Luo, R. Chugh, B.C. Biller et al., Electronic applications of flexible graphite. *J. Electron. Mater.* **31**(5), 535–544 (2002). doi:10.1007/s11664-002-0111-x
14. ASTM Standard D4935-10, in *Standard Test Method for Measuring the Electromagnetic Shielding Effectiveness of Planar Materials*
15. C. Jin, X.Y. Fan, Y. Li et al., Multi-technique characterizations of main elements in the vehicle exhaust particles collected in a tunnel in Shanghai. *Nucl. Sci. Tech.* **22**, 205–211 (2011)
16. W. Liu, J. Yang, Y.A. Huang et al., The Mössbauer investigation in iron nitride/expanded graphite. *Nucl. Tech.* **36**, 010501 (2013). (in Chinese)

17. Y.V. Baldokhin, V.V. Tcherdyntsev, S.D. Kaloshkin et al., Transformations and fine magnetic structure of mechanically alloyed Fe–Ni alloys. *J. Magn. Magn. Mater.* **203**, 313–315 (1999). doi:[10.1016/S0304-8853\(99\)00213-9](https://doi.org/10.1016/S0304-8853(99)00213-9)
18. L.Y. Pustov, V.V. Tcherdyntsev, S.D. Kaloshkin et al., Face-centered cubic phase stability and martensitic transformation under deformation in Fe–Ni and Fe–Mn alloys nanostructured by mechanical alloying and high-pressure torsion. *Mater. Sci. Eng. A* **481–482**, 732–736 (2008). doi:[10.1016/j.msea.2006.12.203](https://doi.org/10.1016/j.msea.2006.12.203)
19. D.G. Rancourt, R.B. Scorzelli, Low-spin γ -Fe–Ni(γ_{LS}) proposed as a new mineral in Fe–Ni-bearing meteorites: epitaxial intergrowth of γ_{LS} and tetraenaite as a possible equilibrium state at 20–40 at% Ni. *J. Magn. Magn. Mater.* **150**, 30–36 (1995). doi:[10.1016/0304-8853\(95\)00089-5](https://doi.org/10.1016/0304-8853(95)00089-5)
20. E.D. Santos, J. Gattacceca, P. Rochette et al., Magnetic hysteresis properties and ^{57}Fe Mössbauer spectroscopy of iron and stony-iron meteorites: implications for mineralogy and thermal history. *Phys. Earth Planet. Inter.* **242**, 50–64 (2015). doi:[10.1016/j.pepi.2015.01.004](https://doi.org/10.1016/j.pepi.2015.01.004)
21. B. Liu, R. Huang, J. Wang et al., Mössbauer investigation of Fe–Ni fine particles. *J. Appl. Phys.* **85**, 1010–1013 (1999). doi:[10.1063/1.369222](https://doi.org/10.1063/1.369222)